Draft:

Normalizing the Behavior of Unsaturated Granular Pavement Materials

Report Prepared for

California Department of Transportation

By

Andrew C. Heath, Juan M. Pestana, John T. Harvey and Manuel O. Bejerano

March, 2004

University of California

Pavement Research Center

Institute of Transportation Studies

1353 South 46^{th} Street

Richmond, CA 94804-4603

Executive summary

One of the important components of a flexible pavement structure are granular material layers. The unsaturated granular pavement materials (UGPMs) in these layers influence stresses and strains throughout the pavement structure, and can have a large effect on asphalt concrete fatigue and pavement rutting, which are two of the primary failure mechanisms for flexible pavements. The behavior of UGPMs is highly dependent on water content, but this effect has been traditionally difficult to quantify using either empirical or mechanistic methods.

This report presents a mechanistic framework for normalizing the behavior of UGPMs within the range of water contents, densities, and stress states likely to be encountered under field conditions. Both soil suction and generated pore pressures are calculated and compared to applied confinement under typical field loading conditions. The framework utilizes a new soil suction model that has three density-independent parameters, and can be determined using conventional triaxial equipment that is available in many pavement engineering laboratories. The suction model can be included with an effective stress constitutive model to determine the response of UGPMs under different loading conditions.

TABLE OF CONTENTS

FIGURES

1 INTRODUCTION

Effective stress in the presence of more than one pore fluid (liquid or gas) is more complicated than the situation where only one pore fluid is present. The behavior of completely dry and completely saturated materials is well understood, but the understanding of the unsaturated case is not as advanced. The pore fluid in granular pavement materials is normally a two phase system consisting of water and air, while other geotechnical engineering applications could include additional gas or liquid phases.

Water content has been shown to have a large effect on granular pavement material response (e.g. Theyse (2000)), but attempts to quantify this effect have mainly been through empirical methods. This document presents a mechanistic framework for normalizing the response of unsaturated granular pavement materials (UGPMs) that can be used in conjunction with an effective stress constitutive model to determine the response of UGPMs under typical field loading conditions. Although this is aimed specifically at UGPMs, the framework can be extended to other geotechnical applications where small deformations are anticipated. The framework is validated using laboratory test data from typical Caltrans Class 2 virgin aggregate base (AB) and recycled aggregate base (RAB) materials.

2 PAVEMENT SATURATION CONDITIONS

Soil saturation (S_w) is defined as:

$$S_w = \frac{V_{v,w}}{V_v} = \frac{w\,G_s}{e} \quad : \quad 0 \leq S_w \leq 1 \tag{2.1}$$

where e is the void ratio, w is the gravimetric water content and G_s is the ratio of the soil particle density to water density. Gravimetric water contents in UGPMs are usually below 10% by mass of dry material, and dry soil unit weights ($\gamma_{s,d}$) are typically between 2.0 and 2.3 (dry density of between 2.0 and 2.3 times that of water). The water saturation at different densities and water contents is illustrated in Figure 2, based on a G_s of 2.72. Included with the saturation curves is a typical compaction curve for the virgin aggregate base (AB) material used for this research (compaction according to CTM-216 (CTM, 2000)).

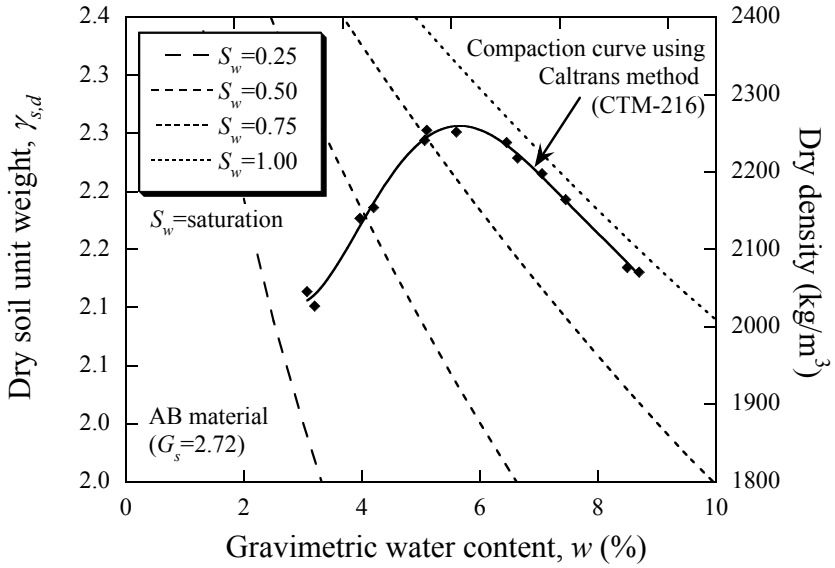

Figure 2.1: Relationships between density, water content and saturation

3 THEORETICAL BASIS

3.1 Effective stress for unsaturated soils

The behavior of unsaturated soils is more complex than the completely saturated or completely dry case because of the difference in compressibility of the pore fluid phases, and because of the internal matric suction caused by water surface tension on a curved interface. For mathematical simplicity, the proposed framework uses an additive approach with the pore air pressure calculated using the pore fluid compressibility, and the pore water pressure calculated using the matric suction and the pore air pressure. This approach requires a modified effective stress relation that was originally proposed by Bishop (1959), and includes the net normal stress $(\sigma - u_a)$ and matric suction $(u_a - u_w)$ as two stress state parameters:

$$\begin{aligned} \sigma' &= (\sigma - u_a) + \chi_w(u_a - u_w) \\ &= (\sigma - u_a) + p_{suc} \end{aligned} \tag{3.1}$$

where σ' is the effective stress, σ is the total stress, χ_w is Bishop's parameter, u_a and u_w are the pore air and pore water pressures, and $p_{suc} = \chi_w(u_a - u_w)$ is the effective suction confinement. According to conventional geotechnical practice, only normal stresses are influenced by pore pressures, and the pore fluid cannot support shear. Equation 3.1 is used by Craig (1992), Khalili and Khabbaz (1998) and Zienkiewicz et al. (1999), but other researchers (e.g. Muraleetharan and Wei (1999)) have shown that Equation 3.1 is valid only under certain conditions, mainly because χ_w depends primarily on the saturation, but also on the material, compaction procedures and stress path. This parameter has the same limits as saturation ($0 \leq \chi_w \leq 1$) and is equal to the saturation for the completely dry and completely saturated cases. The relationship between S_w and χ_w for a number of materials is illustrated in Figure 3.1.

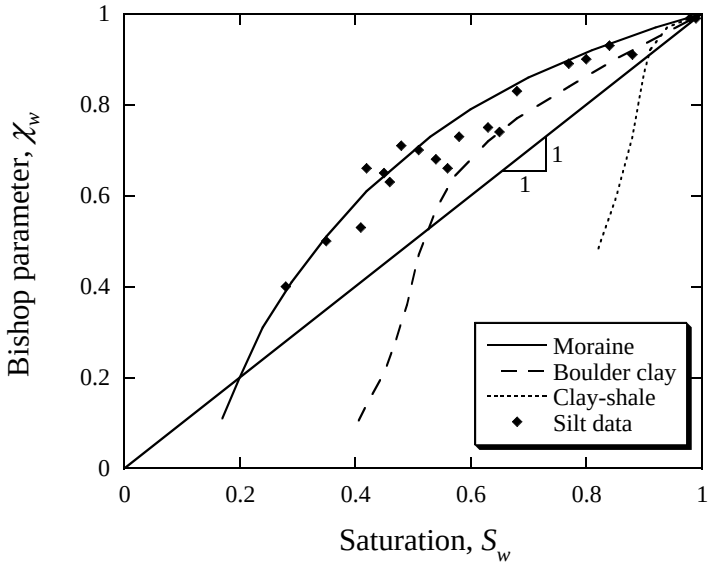

Figure 3.1: Relation between S_w and χ_w for some materials (Blight, 1961; Donald, 1961)

There is a lack of data at very low saturation, and the form of the relation in this range is not well understood. This is of little consequence to UGPM modelling as these low saturation levels are unlikely to be encountered under field conditions. In order to obtain p_{suc} for an unsaturated soil (Equation 3.1), χ_w from Figure 3.1 must be multiplied with $(u_a - u_w)$, ensuring $p_{suc} \leq (u_a - u_w)$.

3.2 Matric suction

3.2.1 Components of soil suction

The matric suction is the component of total soil suction equal to the difference in air and water pressure, generated by water surface tension on a curved interface. This matric suction is what allows sand castles to stand with vertical slopes while the sand is damp, but not when it is completely saturated or completely dry. Total soil suction is made up of the matric and osmotic components:

$$\psi = (u_a - u_w) + \pi \tag{3.2}$$

where ψ is the total soil suction and π is the osmotic suction. The osmotic suction has negligible effect on effective stress, and the matric suction is therefore the portion of total suction influencing effective stress in soils (Fredlund and Rahardjo, 1993).

The relation between matric suction and water content is referred to as the soil-water characteristic curve. Although, there is hysteresis in the soil-water characteristic curve between wetting and drying cycles, this is typically ignored in geotechnical engineering applications. This approach may not, however, be acceptable for pavement engineering applications where near-surface confining stresses are low. An example of a soil-water characteristic curve for a fine sand, showing the hysteresis observed during wetting and drying cycles is illustrated in Figure 3.2 (Gonzalez and Adams, 1980).

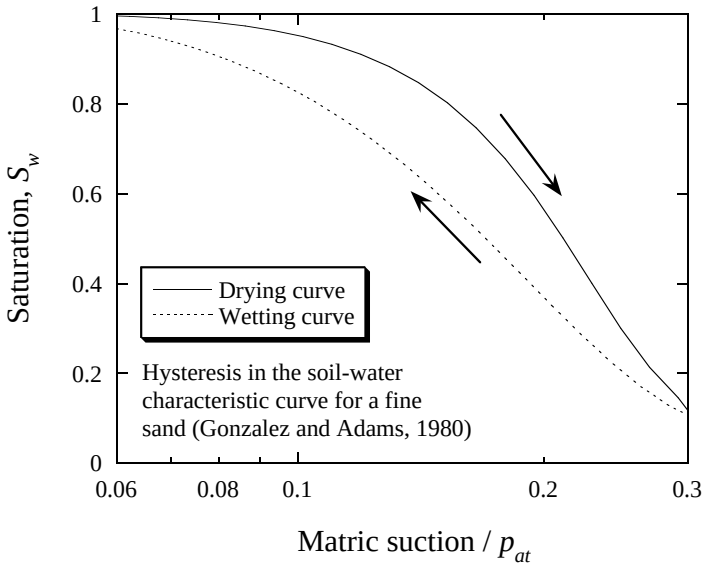

Figure 3.2: Hysteresis in the soil-water characteristic curve (Gonzalez and Adams, 1980)

The shape of the soil-water characteristic curve is highly dependent on the material type and Figure 3.3 shows typical curves for different soils (Fredlund, 2000).

A number of equations have been proposed to describe the soil-water characteristic curve. An example is the empirical equation proposed by Van Genuchten (1980) that requires only

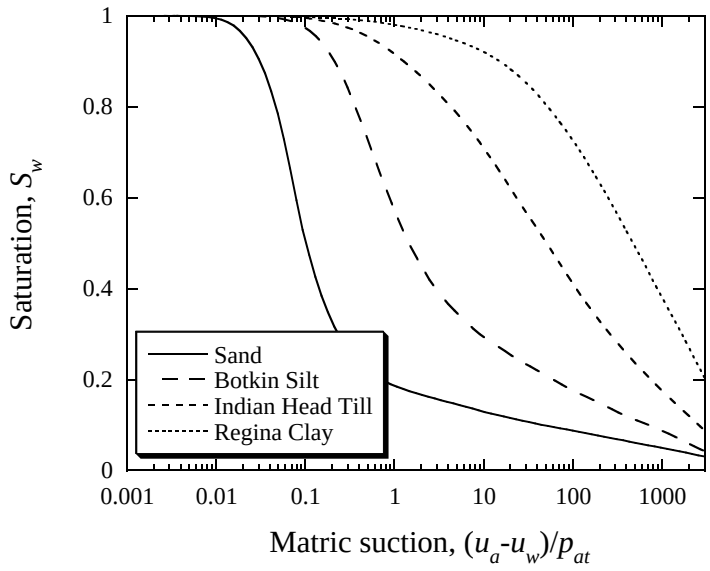

Figure 3.3: Soil-water characteristic curves for some materials (Fredlund, 2000)

three parameters, and can be easily re-written to give a closed form solution for either water content as a function of matric suction, or matric suction as a function of water content. It gives similar results to other, more complicated models within the range of saturation likely for UGPMs:

$$(u_a - u_w)/p_{at} = v_1 \ ({S_w}^{v_2} - 1)^{v_3} \tag{3.3}$$

where p_{at} is atmospheric pressure and v_{1-3} are regression constants.

3.2.2 Suction measurement

It is fairly inexpensive to obtain the soil-water characteristic curve experimentally using a variety of techniques, but some of these methods require specialized equipment (Fredlund and Rahardjo, 1993). The simplest is the filter paper method that uses the principle that suction in a piece of filter paper (usually Whatman #42) and the soil will achieve equilibrium if placed together in a sealed container. If the filter paper is placed in contact with the soil the matric suction is obtained, and if the filter paper and soil are not in contact (but still in the same

airtight container), total suction is measured. After achieving equilibrium, the water content of the soil and filter paper are obtained and the suction in the soil can be calculated using a relation between filter paper water content and suction. Approximate, bi-linear suction versus water content relationships for Whatman #42 and some other filter papers have been determined (Swarbrick, 1995). While the principle and test procedure for the filter paper method are fairly simple, it is not particularly accurate for measuring either matric or total suction.

There are empirical relations that link matric suction to material properties (e.g. Fredlund et al. (2000)), but these have not been sufficiently verified for UGPMs, where matric suction could supply a large portion of the effective confinement.

3.2.3 Effect of density

Soil suction has been shown to be largely independent of material density in the medium to low saturation range. For this reason, the soil-water characteristic curve is often presented as a function of w instead of saturation (as shown in Figure 3.3). Total and matric suction as a function of water content for a low plasticity glacial till (Plasticity Index = 16.9), compacted to different densities ($\gamma_{s,d}$) is illustrated in Figure 3.4.

While the soil-water characteristic curve is independent of density at medium to low saturation, this is not the case at high saturation levels as denser samples will become completely saturated ($(u_a - u_w) \rightarrow 0$) at lower water contents than for looser samples.

The relation proposed by Van Genuchten (1980) (Equation 3.3) and most other equations describing the soil-water characteristic curve are based on saturation and thereby ensure $(u_a - u_w) \rightarrow 0$ as $S_w \rightarrow 1$. While this allows realistic modelling of behavior at high saturation levels, the dependence on saturation results in a density dependence in the mid to low saturation range, and the model regression parameters are therefore only valid for a certain density. This

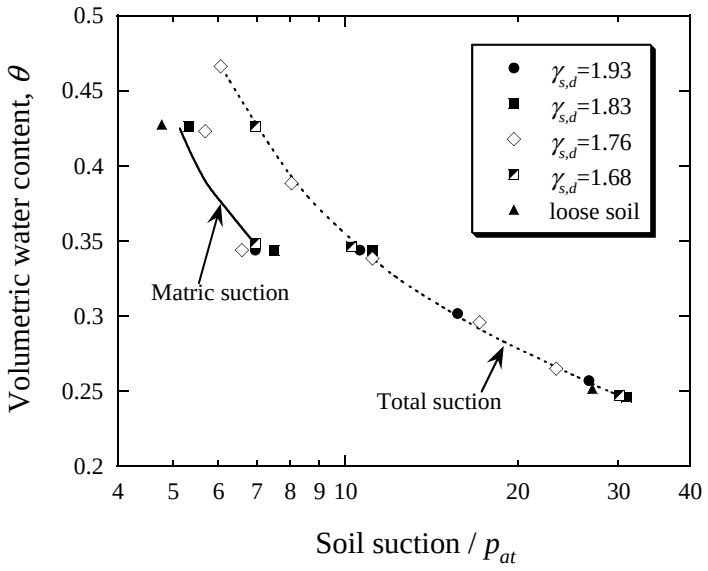

Figure 3.4: Soil suction at various densities for a low plasticity glacial till (Krahn and Fredlund, 1972)

is a limitation of existing models, and a density-independent relationship is therefore proposed (see later).

3.3 Compressibility of pore fluid

The pore fluid in an UGPM is usually a mix of air and water. While water is often considered incompressible in geotechnical engineering, this is not strictly correct. The compressibility of water is, however, very low compared to that of air in the range of pressures in pavement and most geotechnical applications. If the pore fluid drains freely, its compressibility is not important as any generated pore pressures will dissipate.

For undrained loading, pore air pressures will be generated if there are volumetric deformations and the change in pore air pressure can then be calculated using the change in pore air volume and Boyle's law for an ideal gas. The volume of air dissolved in the water can be calculated using Henry's law and is approximately 2% of the volume of water at 20°C (Moran and

Shapiro, 1996). Increasing the air pressure will increase the mass of air dissolved in the water. Because of the low pore air pressures and small volumetric deformations during a single load cycle on UGPMs, it is possible to use a simplified approach where water is considered incompressible relative to air. For undrained loading of an unsaturated soil at constant temperature, Boyle's law can be written as:

$$u_a = (u_{ao} + p_{at})\frac{e_o + (h-1)wG_s}{e + (h-1)wG_s} - p_{at} \tag{3.4}$$

where u_{ao} is the initial pore air pressure, e_o is the initial void ratio, and h is the volumetric coefficient of solubility (approximately 0.02 at 20°C (Moran and Shapiro, 1996)). For undrained loading, the value for u_a from Equation 3.4 can be substituted into Equation 3.1 to obtain the effective stress. As volumetric strains depend on effective stress and vice-versa, an iterative solution is required.

As $wG_s \rightarrow e$ (full saturation), $(u_a - u_w) \rightarrow 0$ (i.e. $u_a \rightarrow u_w$), and the effective stress relationship can be written in its conventional form for saturated soils:

$$\sigma' = \sigma - u_w \tag{3.5}$$

The transition from unsaturated conditions (Equation 3.1) to fully saturated conditions (Equation 3.5) indicates an immediate increase in pore pressures for samples undergoing compressive volumetric strains. While a large increase is noted during laboratory testing of soils approaching full saturation, it is not immediate. This is likely a result of sample scale where the pore air is not uniformly distributed in real samples close to full saturation. This is of little consequence for pavement engineering applications as a conservative estimate of full saturation should be used if saturation levels approach 1.

4 NORMALIZING THE RESPONSE OF UNSATURATED GRANULAR PAVEMENT MATERIALS

Normalizing the response of UGPMs will enable calculation of effective stress at a range of water contents. This can then be included with an effective stress constitutive model to predict behavior of UGPMs under field loading conditions.

4.1 Effective stress

In order to normalize the response of the material, the Bishop's effective stress relationship for unsaturated soils (Equation 3.1) is used.

4.1.1 Suction

Most pavement engineering laboratories do not have the equipment required to directly measure the soil-water characteristic curve. Even if this curve is known, the the effective suction confinement (p_{suc}) is required rather than the matric suction and this requires χ_w (Figure 3.1) to be known as a function of saturation, stress path and density. The hysteresis in the soil-water characteristic curve (Figure 3.2) also limits the accuracy of this approach. Because all these factors increase uncertainty in effective stress prediction, a procedure is proposed where p_{suc} is back-calculated from monotonic shear tests on soils. The relationship between water content and p_{suc} can then be included with an effective stress constitutive model to predict the behavior of UGPMs at different water contents and stress states.

Khalili and Khabbaz (1998) summarized a number of laboratory studies on different materials that indicated the relation between χ_w and $(u_a - u_w)$ is linear in log-log space at medium to low saturation levels. If this relation is combined with the Van Genuchten (1980) equation

for the soil-water characteristic curve (Equation 3.3), it indicates the relation between w and p_{suc} (or S_w and p_{suc}) is also linear in log-log space at intermediate and low saturation levels. The following equation is therefore proposed for p_{suc}:

$$\frac{p_{suc}}{p_{at}} = \frac{wG_s}{e}\, n_1 \left(\frac{1}{(wG_s)^{n_2}} - \frac{1}{e^{n_2}} \right)^{n_3/n_2} \tag{4.1}$$

where n_{1-3} are regression parameters. Equation 4.1 has density-independent model parameters and predicts a linear relation in log-log space at intermediate and low saturation levels, and includes a smooth transition to $p_{suc} = 0$ at full saturation. Data for the Bishop (1959) model (Equation 3.1) was obtained by multiplying the matric suction with the χ_w data for the silt materials in Figures 3.3 and 3.1 and this is compared to Equation 4.1 in Figure 4.1. Although it is possible to present this data in terms of saturation, in order to calculate the model parameters and to present the data in a form consistent with the rest of this document, an assumption of $e = 0.5$ was used. As shown, the proposed density-independent model (Equation 4.1) has a very good correlation with the data, and confirms the linear relation between w and p_{suc} at intermediate and low saturation levels.

As shown, Equation 4.1 does not require $(u_a - u_w)$ or χ_w, but instead calculates the combined effect. It is not possible to directly separate these two parameters, but an approximate soil-water characteristic curve can be calculated by assuming $\chi_w = S_w$, leading to the following relationship:

$$\frac{(u_a - u_w)}{p_{at}} \approx n_1 \left(\frac{1}{(wG_s)^{n_2}} - \frac{1}{e^{n_2}} \right)^{n_3/n_2} \tag{4.2}$$

Equation 4.2 describes a family of approximate soil-water characteristic curves for different densities (different values of e), as illustrated in Figure 4.2. The model is characterized by a limiting suction curve (LSC) that is able to describe the density independent matric suction in the mid to low saturation ranges (Figure 3.4), but still ensures the matric suction tends

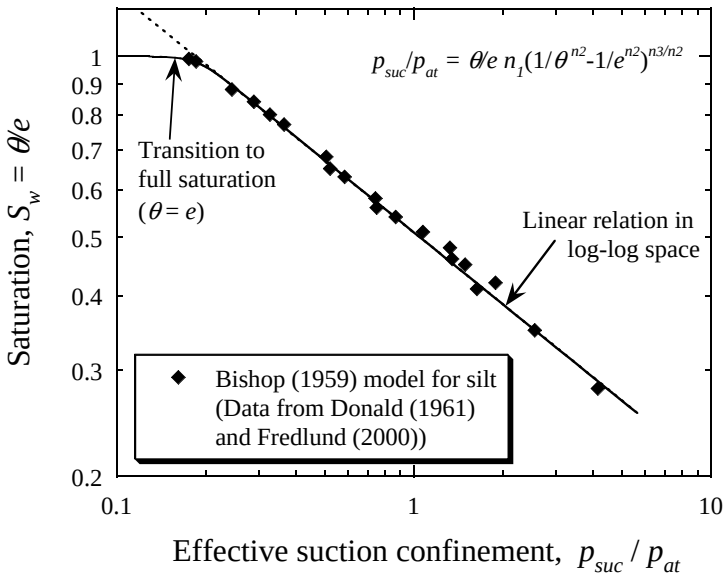

Figure 4.1: Effective suction confinement as a function of water content using the Bishop (1959) and proposed density-independent models

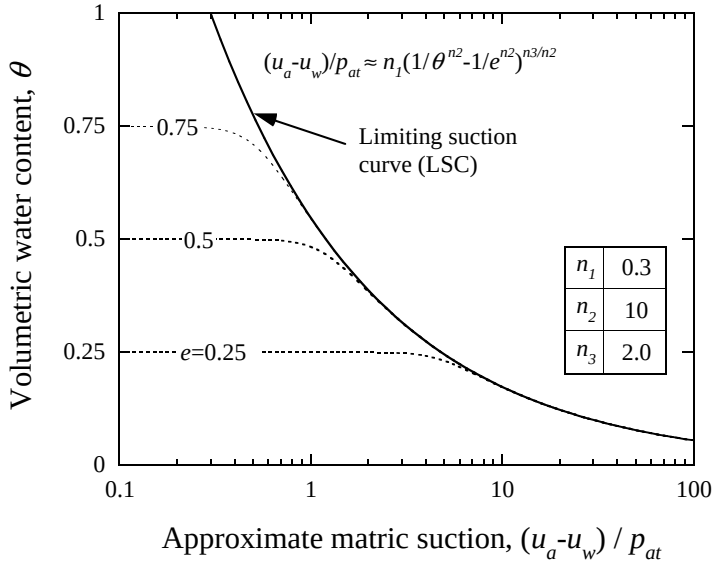

Figure 4.2: Density independent approximate soil-water characteristic curve

to zero as full saturation is approached. This overcomes the limitation of density dependence of previous models (e.g. Equation 3.3 (Van Genuchten, 1980)), enabling the the behavior at different water contents and densities to be quantified without requiring new model parameters.

Assuming e, G_s and w are known, only three parameters (n_{1-3}) are required to determine

the effective suction confinement over the range of densities and moisture conditions likely to be encountered in UGPMs. The approximate matric suction tends to zero as $wG_s \rightarrow e$ (full saturation), and to the unique LSC as w decreases (see Figure 3.4). The LSC describes the maximum suction at a particular water content, regardless of density. The effect of n_{1-3} is best visualized in log-log space, instead of the log-linear space often used for the soil-water characteristic curve, and this is illustrated in Figure 4.3.

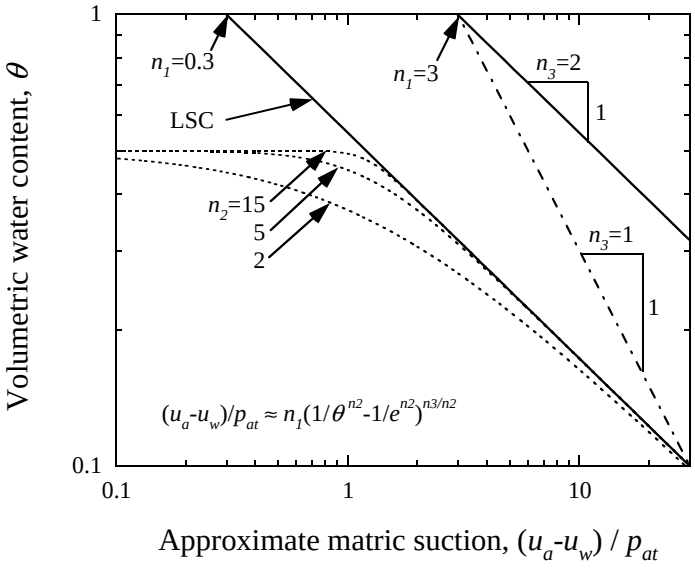

Figure 4.3: Effect of parameters n_{1-3} on approximate soil-water characteristic curve

As shown, the parameter n_1 gives the intercept of the LSC at wG_s=1, and varying this parameter shifts the curve left or right. The parameter n_3 gives the slope of the LSC in log-log space with the value of n_3 equal to the ratio of log scale changes in matric suction to log scale changes in wG_s. The parameter n_2 controls the transition to full saturation with Equation 4.2 predicting a bi-linear relation as $n_2 \rightarrow \infty$.

As mentioned earlier, Equation 4.1 is a simplified form of the Bishop (1959) equation and therefore has the same limitation of stress path dependence. Back-calculating p_{suc} from laboratory shear test data does have a number of advantages over the conventional approach of

measuring $(u_a - u_w)$ and χ_w, and multiplying them to obtain p_{suc}. If the laboratory tests are performed at similar conditions to those expected in the field, the back-calculation procedure will minimize the effect of hysteresis in the soil-water characteristic curve, and minimize the effect of the stress path dependence of χ_w. In addition, no specialized laboratory equipment is required for the measurement of $(u_a - u_w)$ and χ_w.

4.1.2 Generated pore pressures

No pore air pressure will be generated during drained loading, and the pore air pressures generated during undrained loading can be calculated using Equation 3.4. This requires measurement of volumetric strains, a procedure that is complicated if monotonic shearing results in volume changes along a single failure plane. Although pore air pressures generated during monotonic shearing of UGPMs are likely to be low, it is recommended that laboratory testing be performed under drained conditions to minimize their effect.

4.2 Laboratory testing

In order to normalize the unsaturated response, it is necessary to prepare samples where the only difference is the variation in moisture content and density. This presents some difficulty as the easiest method of preparing samples at different water contents is to compact them at the required water content.

The difference in soil fabric (dispersed or flocculated) between cohesive materials compacted wet and dry of the optimum water content (w_{opt}) has been well documented (e.g. Seed et al. (1962)). Although the virgin aggregate base (AB) material used for this research is non-plastic, permeability tests indicated fabric differences for samples compacted wet or dry of w_{opt} (Russo, 2000). The monotonic and dynamic triaxial testing performed as part of this research also

indicated strong evidence of fabric differences for the AB material where small changes in w around w_{opt} resulted in large changes in strength and stiffness. These fabric differences were not noted in the recycled aggregate base (RAB) material, the other material used for this research. The AB samples with a dispersed fabric were therefore taken as one sample group and the samples with a flocculated fabric were taken as another.

4.2.1 Monotonic shear

The Mohr-Coulomb failure criteria is probably the most popular method of determining the shear strength of soils. This is a simple model for predicting peak shear strength and is only used for illustrative purposes:

$$\tau_{ff} = c' + \sigma'_n \tan\phi' \tag{4.3}$$

where τ_{ff} is the shear strength on the failure plane, c' is the effective cohesion, σ'_n is the effective stress normal to the shear plane, and ϕ' is the effective friction angle. The Mohr-Coulomb criteria is not an accurate representation of peak shear strength for a number of reasons. One of these is that many newly deposited soils can be considered to have no true cohesion (i.e. $c' = 0$) which is in line with Coulomb's original work (Heyman, 1972), and that of many other researchers (e.g. Schofield (1998); Pestana and Whittle (1999)). Apparent cohesion can come from a number of sources, including matric suction.

A second reason for the inaccuracy of the Mohr-Coulomb criteria is that experimental evidence has shown ϕ' is not constant for dense granular materials at low confining stresses. The following equation fits laboratory shear test data on compacted granular soils (Duncan et al., 1980):

$$\phi' = \phi'_o - \Delta\phi' \log\left(\frac{\sigma'_3}{p_{at}}\right) \tag{4.4}$$

where ϕ'_o is the effective friction angle at 1 atm confining pressure, $\Delta\phi'$ is the change in effective friction angle with confining stress, and σ'_3 is the minor principal effective stress (effective confining stress in a triaxial compression test).

The monotonic shear testing for this research was performed under drained conditions and no significant pore air pressures were generated during loading. As a result, σ'_3 in Equation 4.4 is taken as the sum of the total confining stress (σ_3) and p_{suc} from Equation 4.1. This requires a total of five unknown parameters (ϕ'_o, $\Delta\phi'$ and n_{1-3}) to determine the monotonic shear strength of an unsaturated soil at any given density and soil fabric. As the matric suction (Equation 4.2) is independent of density but the friction angle depends on sample density and soil fabric, two parameters (ϕ'_o and $\Delta\phi'$) are required at each additional density or soil fabric.

4.2.2 Resilient response

Dynamic testing to determine the resilient properties of UGPMs can be performed using the Strategic Highways Research Program (SHRP) P46 protocol (FHWA, 1996). This test involves applying different amplitude haversine shaped deviatoric pulses at different confining stresses. Because loading is primarily in the elastic range and there is a short (100 ms) loading time and longer (900 ms) rest time between pulses, loading can be assumed as undrained during the pulse application, but drained (pore pressures allowed to dissipate) between successive loads. It is currently not possible to accurately measure generated pore pressures during the 100 ms load pulses in a P46 test, and the generated pore pressures were therefore calculated using Equation 3.4 and used to determine the effective stress. The Uzan (1985) model for resilient modulus of UGPMs can be written in a dimensionless form:

$$\frac{M_r}{p_{at}} = k_1 \left(\frac{p'}{p_{at}}\right)^{k_2} \left(\frac{q}{p_{at}}\right)^{k_3} \tag{4.5}$$

where M_r is the resilient modulus, $p' = (\sigma'_1 + \sigma'_2 + \sigma'_3)/3$ is the mean effective stress, $q = \sigma_1 - \sigma_3$ is the deviatoric stress, and k_{1-3} are regression constants. There are other simple bulk stress models that ignore the deviatoric component (e.g. Dehlen and Monismith (1970); Hicks and Monismith (1971)), but these do not provide as accurate a description of resilient behavior.

For undrained loading during a P46 test, the mean effective stress is calculated using the applied total stress, effective suction confinement (Equation 4.1) and generated pore air pressures (Equation 3.4):

$$p' = \frac{\sigma_1 + \sigma_2 + \sigma_3}{3} + p_{suc} - u_a \tag{4.6}$$

Each P46 test has 15 blocks with different confining and deviatoric stresses, and the model in Equation 4.5 has only four unknown parameters (k_{1-3} and p_{suc}). If the suction parameters for Equation 4.1 are already known from monotonic shear tests, one P46 test is required to determine the response of a material for a given density and soil fabric. If the suction parameters are not known, it is possible to use P46 tests at a minimum of three water contents to calculate n_{1-3} and the approximate soil-water characteristic curve. Because of the high variability in small strain stiffness measurements on UGPMs (Ansell, 1977; Chan and Brown, 1991; Bejarano et al., 2002), the use of monotonic shear data is preferred for the calculation of soil suction.

5 EXPERIMENTAL VALIDATION

The testing preformed as part of this research is summarized in Bejarano et al. (2002) and Heath (2002), and only selected results are used for validation of the normalizing framework.

5.1 Monotonic shear

5.1.1 Total stress envelope

Conventional total stress analysis using the Mohr-Coulomb failure criteria (Equation 4.3) assumes some apparent cohesion (c). Because of the small range in confining stress, the total friction angle ϕ was assumed constant and total stress failure envelopes for the AB material at 95% and 100% compaction according to CTM-216 are illustrated in Figure 5.1.

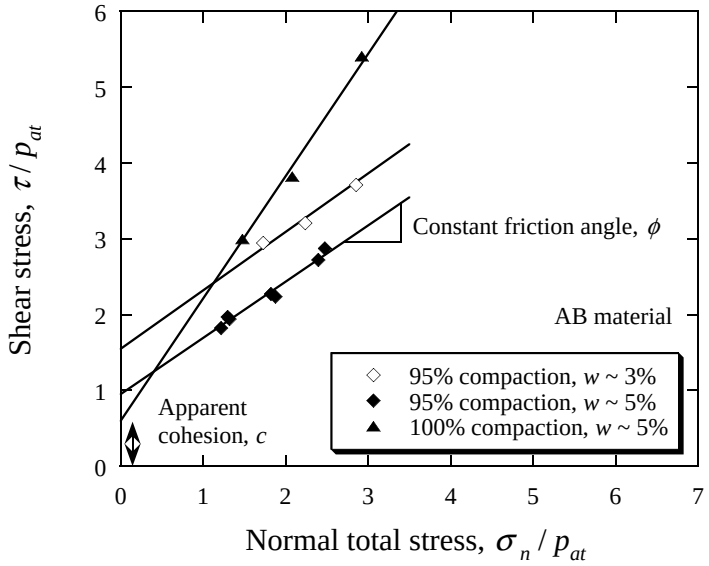

Figure 5.1: Total stress failure envelopes for AB samples with flocculated structure

The samples in Figure 5.1 all have a flocculated structure, and are separated based on a target w of 3% and 5% for 95% compaction, and a target w of 5% for 100% compaction. To enable easy visualization of the data, the points in the figure are the failure points (τ_{ff} and σ_n)

calculated using the failure envelopes shown. These failure points indicate the position on the Mohr circle where the circle has the same gradient as the failure surface.

5.1.2 Calculation of suction

In order to calculate the effective stress under unsaturated conditions, a regression analysis was performed using the monotonic triaxial test data for the AB and RAB materials. This enabled the friction angle (ϕ'_o and $\Delta\phi'$) at each density and soil fabric, and the three suction parameters for the materials (n_{1-3}) to be determined. The approximate back-calculated soil-water characteristic curves (Equation 4.2) for the two materials are illustrated in Figures 5.2 and 5.3. The three suction model parameters (n_{1-3}) as well as the two friction parameters at each density and soil fabric (ϕ'_o and $\Delta\phi'$) are included on the figures. As shown, the peak friction angle increases with increasing density and as the fabric moves from a dispersed to flocculated structure.

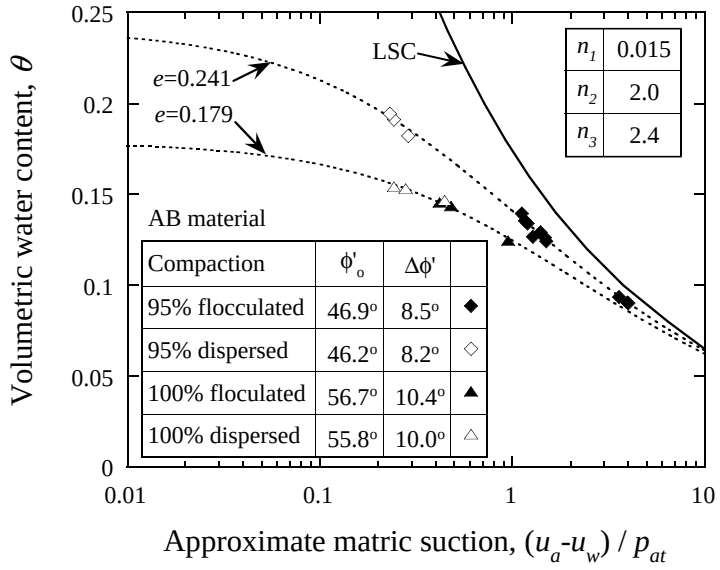

Figure 5.2: Approximate soil-water characteristic curve for AB material

The shape of the approximate soil-water characteristic curves is slightly different to the

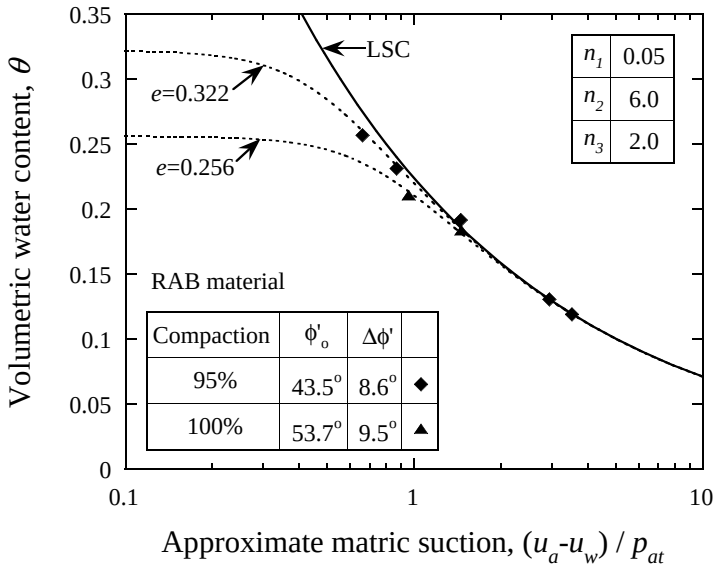

Figure 5.3: Approximate soil-water characteristic curve for RAB material

examples in Figure 3.3, mainly because the void ratio of compacted UGPMs is much lower than that of most other soils, leading to full saturation at lower water contents. The friction parameters are on the high side of the typical values presented by Duncan et al. (1980), and this is also because of the low e of UGPMs. There was some variability in the target compaction water content that would have introduced variability into the total stress envelopes shown in Figure 5.1. The normalizing procedure reduces the variation from incorrect testing moisture contents.

The effective suction confinement is affected by sample density, as illustrated in Figure 5.4 for the AB and RAB materials at 95% and 100% compaction. In this figure the curves are plotted as a function of saturation on a log-log scale to allow easier comparison of the relative shapes.

As shown, p_{suc} for the materials is large compared to the applied confinement during a P46 test (maximum of 1.4 atm), indicating the suction is supplying a major portion of the effective confinement during the test, which is performed at typical field stress states (FHWA,

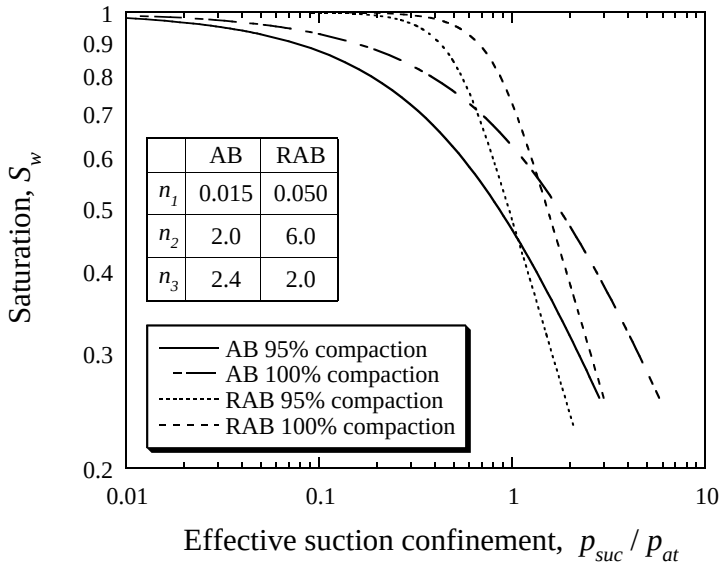

Figure 5.4: Effective suction confinement at different relative compaction levels

1996). The curve for the AB material is flatter than for the RAB material, indicating the AB performance is more sensitive to changes in water content. The increased p_{suc} with increased density is because the soil-water characteristic curve is largely independent of density (Figure 3.4), but χ_w is dependent on density through the dependence on saturation (Figure 3.1). This is predicted by Equation 4.1 and from the test data, but is counterintuitive as an increase in density at constant water content results in an increase in saturation. At constant density, an increase in saturation results in a decrease in matric suction.

5.1.3 Effective stress envelope

The effective confinement for the monotonic triaxial testing was increased by adding p_{suc} (Equation 4.1) to the applied confining stress, and calculating new effective stress failure envelopes. This is illustrated in Figure 5.5 for the same AB samples shown in Figure 5.1. The difference in the total stress envelopes in Figure 5.1 (includes c) and the effective stress envelopes in Figure 5.5 (that include suction and c=0) is evident.

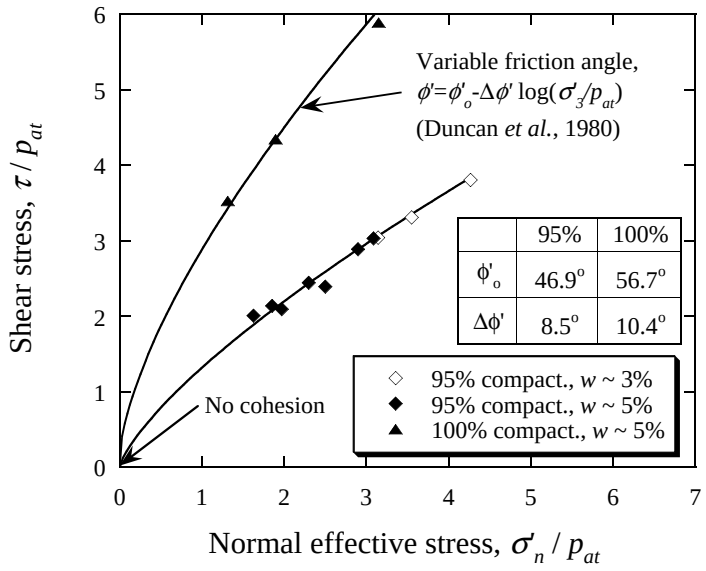

Figure 5.5: Effective stress failure envelopes for AB samples with flocculated structure

The envelopes in Figure 5.5 go through the origin because the framework assumes all effective cohesion is provided by matric suction. The model correlates well with the data, indicating the assumption of $c' = 0$ is reasonable for these materials.

5.1.4 Number of tests

If the peak shear strength envelopes at three densities and three moisture contents are required, significantly less tests are required for the framework outlined here than for a conventional total stress approach. If the total stress approach is used with a non-linear failure envelope, the minimum number of tests required is 3 shear parameters $\times$ 3 densities $\times$ 3 moisture contents = 27 samples. Slight variations in compaction moisture content could affect results and some tests may have to be repeated.

If the normalized approach is used to back-calculate the shear strength and suction parameters, and there is no effect of soil fabric, the number of tests decreases to 2 shear parameters $\times$ 3 densities + 3 suction parameters = 9 samples. If there is evidence of soil fabric, this will

increase to 2 shear parameters × 3 densities × 2 fabrics + 3 suction parameters = 15 samples, still significantly less than that required for the total stress approach. In addition, any variations in sample moisture content can be easily accommodated without having to repeat tests.

The normalized approach provides a mechanistic framework for determining the response at moisture contents other than those used in the testing, and provides a framework for other aspects of material behavior, such as for determining the resilient response.

5.2 Resilient response

5.2.1 Generated pore pressures

As the volumetric behavior during the P46 dynamic testing was monitored using the on-sample instrumentation, it was possible to back-predict u_a using Equation 3.4 and a summary of u_a divided by p_{suc} is presented in Figure 5.6. Because u_a changes through the different test blocks while p_{suc} remains constant, only the peak value of u_a from all the test blocks is given.

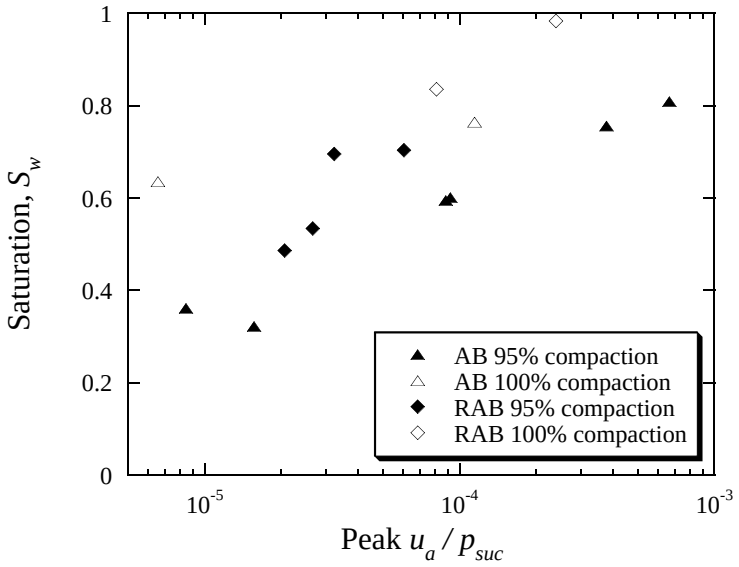

Figure 5.6: Ratio between u_a and p_{suc} during P46 testing

As expected, the samples with a higher S_w generally had a higher u_a, although these were still very low compared to p_{suc} (less than three orders of magnitude (0.1%) in all cases). As the samples approach full saturation, the pore pressures will increase and the suction will decrease, leading to softer, weaker samples. Because u_a is much smaller than p_{suc}, it is likely the generated pore pressures can be ignored for all practical pavement engineering purposes, provided $S_w < 0.95$. Because of the low accuracy of saturation (w and e) estimates, a conservative estimate of full saturation is recommended for $S_w > 0.95$.

5.2.2 Comparison with laboratory test results

As validation for the framework under different loading conditions, predictions using the Uzan model (Equation 4.5) are compared with the measured resilient modulus for samples with $w \approx 3\%$ and $w \approx 5\%$ in Figure 5.7. For the first set of data, a total stress approach was used (soil suction was ignored) and the Uzan model parameters were determined using a regression analysis on all the data, regardless of water content. For the second data set, p_{suc} was included using the suction model parameters calculated from the monotonic triaxial test data (Figure 5.2), and performing a regression analysis to obtain new Uzan model parameters.

If suction is ignored, the samples cannot be considered to come from the same sample group and the coefficient of correlation between the data and model predictions is only 0.25. In order to provide a reasonable prediction of response, the total stress approach requires testing and model parameters to be calculated at each water content. The inclusion of matric suction produces a much improved estimate of response, and the coefficient of correlation increases to 0.69 and is limited more by the variation in resilient modulus results (Bejarano et al., 2002) than the changes in water content. If the effective suction confinement relation is known from monotonic testing, it is only necessary to perform one P46 test for each sample group (different

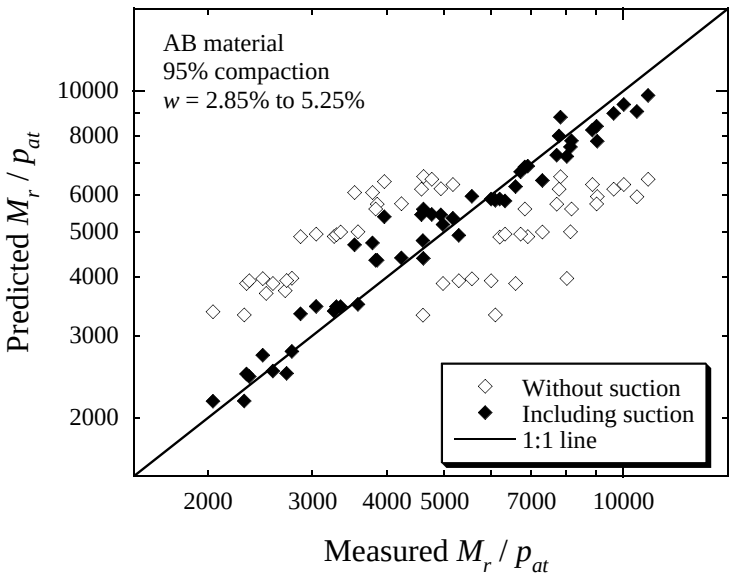

Figure 5.7: Comparison of measured and predicted resilient modulus

density or soil fabric) to obtain the Uzan model parameters. Because of the variability in P46 test results, it is recommended that more than one test be performed.

6 LARGE STRAIN BEHAVIOR

While the procedure outlined above can be used to normalize the behavior of UGPMs at low strains, Bishop's additive approach to unsaturated soil effective stress (Equation 3.1) is not applicable to large strain behavior. As UGPMs are unlikely to be sheared to large strains, this section is only included for the interest of readers who wish to use this framework for other geotechnical problems where large strains are anticipated. Figure 6.1 shows the relationship between deviatoric stress (q) and axial strain (ε_a) during monotonic triaxial testing at different total confining stresses (σ_3).

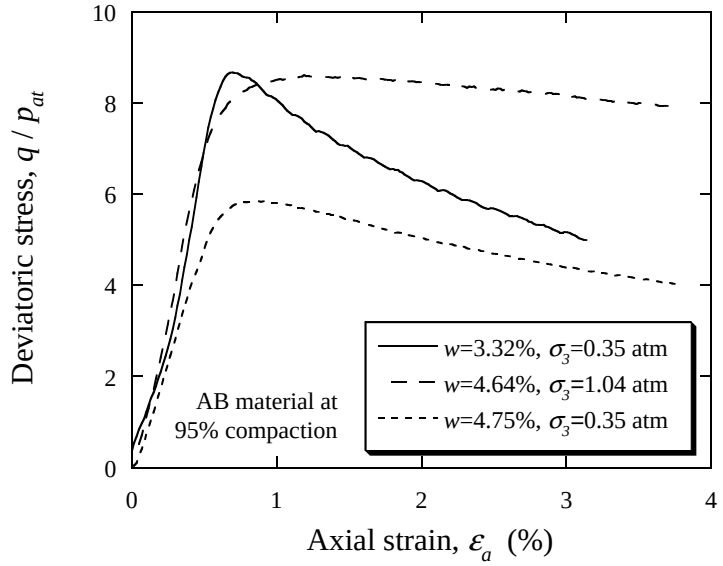

Figure 6.1: Difference in post peak shear behavior for AB samples with different w and σ_3

If p_{suc} from Figure 5.4 is included, the sample with $w = 3.32\%$ and $\sigma_3 = 0.35$ atm, and the sample with $w = 4.64\%$ and $\sigma_3 = 1.04$ atm have similar effective confining stresses. As a result, the peak strengths and small strain stiffness are similar, but the post-peak behavior is very different with the drier sample (large p_{suc} and small σ_3) showing more brittle behavior than the wetter sample (small p_{suc} and large σ_3). The AB samples are well compacted, dense

and under low confinement, resulting in dilation along a single failure plane during large strain shearing. While this dilation will reduce the density and therefore p_{suc} along the failure plane (see Figure 5.4), this does not appear to be the primary cause of the difference in post-peak behavior.

The reduction in density from dilation during shearing would decrease p_{suc} slightly, but the test data indicates a constant residual strength is approached at each σ_3, regardless of w. This can be seen by comparing the graphs for $w = 3.32\%$ and 4.75% and a constant $\sigma_3 = 0.35$ atm. While the tests were stopped before large strain conditions stabilized, it appears as if the two samples are approaching a similar residual strength. The tests were stopped because large radial deformations would have caused additional confinement from the membrane, giving inaccurate results.

The primary cause for the more brittle behavior of the drier samples appears to be because the interface between the pore air and pore water breaks down during large strain shearing. This trend is also noted for the RAB material (Figure 6.2) where three samples with $\sigma_3 \approx 1$ atm approached a similar value of residual strength, even though the peak strength was highly dependent on water content.

The data for both materials indicates that p_{suc} decreases during large strain shearing and the Bishop (1959) additive approach for unsaturated soil effective stress is therefore not applicable under these conditions. As mentioned earlier, this is of little consequence to UGPMs as large strain shearing is unlikely to be encountered under normal field conditions.

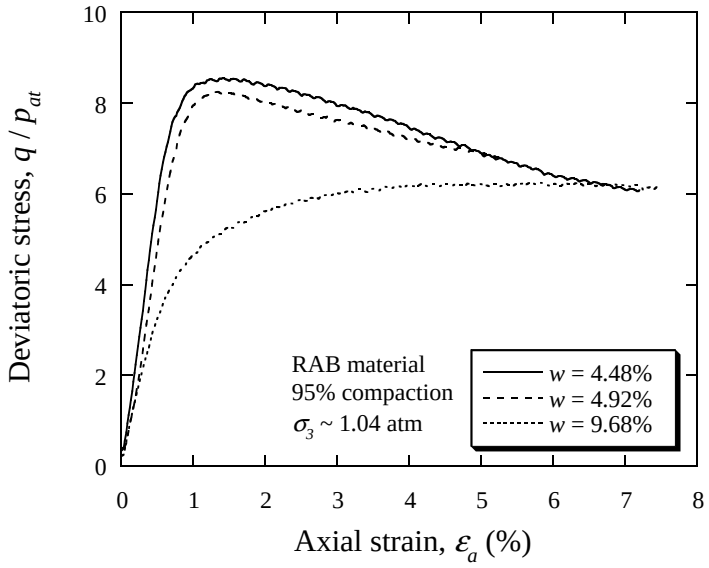

Figure 6.2: Difference in behavior for RAB samples with different w and $\sigma_3 \approx 1$ atm

7 SUMMARY OF PROCEDURE

The procedure for normalizing the behavior of UGPMs is summarized below:

- Perform a minimum of five drained monotonic triaxial shear tests on a soil with constant density and soil fabric. These tests should be performed over a range of water contents.
- Perform a minimum of two monotonic shear tests at each additional density or soil fabric.
- Use the Mohr-Coulomb failure criteria with $c' = 0$, and obtain the two shear parameters at each density and soil fabric, and the three unsaturated model parameters for the soil by performing a regression analysis using the peak shear strengths.

The regression analysis requires the following equations:

$$\begin{aligned} \sin\phi' &= \frac{q_{max}}{2\sigma'_3 + q_{max}} \\ \phi' &= \phi'_o - \Delta\phi' \log\left(\frac{\sigma'_3}{p_{at}}\right) \\ \sigma'_3 &= \sigma_3 + p_{suc} \\ \frac{p_{suc}}{p_{at}} &= \frac{wG_s}{e}\, n_1 \left(\frac{1}{(wG_s)^{n_2}} - \frac{1}{e^{n_2}}\right)^{n_3/n_2} \end{aligned} \tag{7.1}$$

where σ_3 is the applied confining stress in the triaxial cell, q_{max} is the measured deviatoric stress at failure, ϕ'_o and $\Delta\phi'$ are the two shear regression parameters at each density and soil fabric, and n_{1-3} are the three suction regression parameters for the material. Once the material parameters have been obtained, the last line of Equation 7.1 can be used with other effective stress constitutive models for UGPMs.

8 CONCLUSIONS

This chapter presents a mechanistic framework for including unsaturated behavior into granular pavement material constitutive modelling. The effect of both generated pore pressures and soil suction are quantified and compared to the applied total stresses. For the materials tested, the soil matric suction is far more important than the generated pore pressures for determining effective stresses under typical pavement engineering conditions, and the generated pore pressures can be ignored for all practical purposes. The effective confinement from matric suction can exceed the applied confinement in a P46 resilient modulus test, which is performed at stress levels similar to those under field conditions.

The framework back-calculates the effective stress under unsaturated conditions by utilizing triaxial test equipment that is available in many pavement engineering laboratories. The framework is valid for other loading conditions, and can be included into a three-dimensional finite element or other computational code with an effective stress constitutive model. This will enable the effect of soil moisture on pavement behavior to be quantified.

More monotonic and dynamic triaxial tests are required for a conventional total stress approach to granular pavement material modelling than required for the framework presented here. This framework does not sacrifice any accuracy and enables behavior at different water contents to be quantified. Although this method is not applicable to large strain conditions, it has been validated for granular pavement materials at typical field densities and stress states.

REFERENCES

Ansell, P. (1977). *Cyclic simple shear testing of granular material.* Ph. D. thesis, University of Nottingham.

Bejarano, M. O., A. C. Heath, and J. T. Harvey (2002). A low-cost high-performance alternative for controlling a servo-hydraulic system for triaxial resilient modulus apparatus. In *ASTM Symposium On Resilient Modulus Testing for Pavement Components*, Salt Lake City, UT.

Bishop, A. W. (1959). The principle of effective stress. *Tecknish Ukeblad 106*(39), 859–863.

Blight, G. E. (1961). *Strength and Consolidation Characteristics of Compacted Soils.* Ph. D. thesis, University of London.

Chan, W. K. F. and S. F. Brown (1991). Granular bases for heavily loaded pavements. Technical Report PR91019, University of Nottingham, Department of Civil Engineering, Nottingham, UK.

Craig, R. F. (1992). *Soil Mechanics* (5th ed.). London: Chapman and Hall.

CTM (2000). Relative compaction of untreated and treated soils and aggregates. Test CTM-216, Caltrans Engineering Service Center, Transportation Laboratory, Sacramento, CA.

Dehlen, G. L. and C. L. Monismith (1970). Effect of nonlinear material response on the behavior of pavements under traffic. *Highway Research Record 310*, 1–16.

Donald, I. B. (1961). *The Mechanical Properties of Saturated and Partly Saturated Soils with Special Reference to Negative Pore Water Pressures.* Ph. D. thesis, University of London.

Duncan, J. M., P. Byrne, K. S. Wong, and P. Mabry (1980). Strength, stress-strain and bulk

modulus parameters for finite element analysis of stresses and movements in soil masses. Technical Report UCB/GT/80-01, University of California, Berkeley, CA.

FHWA (1996). LTPP materials characterization: Resilient modulus of unbound materials. Protocol P46, U.S. Department of Transportation, Federal Highway Administration. Research and Development, McLean, VA.

Fredlund, D. G. (2000). The 1999 R.M. Hardy lecture: The implementation of unsaturated soil mechanics into geotechnical engineering. *Canadian Geotechnical Journal 37*(5), 963–986.

Fredlund, D. G. and H. Rahardjo (1993). *Soil Mechanics for Unsaturated Soils.* New York: Wiley and Sons.

Fredlund, M. D., D. G. Fredlund, and G. W. Wilson (2000). Prediction of the soil-water characteristic curve from grain size distribution and volume-mass properties. In *NONSAT '97: 3rd Brazilian Symposium on Unsaturated Soils*, Rio de Janeiro, Brazil, pp. 13–23.

Gonzalez, P. A. and B. J. Adams (1980). Mine tailings disposal: I. Laboratory characterization of tailings. Technical report, Dept of Civil Engineering, University of Toronto, Toronto, Canada.

Heath, A. C. (2002). *Modelling unsaturated granular pavement materials using bounding surface plasticity.* Ph. D. thesis, University of California at Berkeley.

Heyman, J. (1972). *Coulomb's Memoir on Statics; An Essay in the History of Civil Engineering.* Cambridge, U.K.: Cambridge University Press.

Hicks, R. G. and C. L. Monismith (1971). Factors influencing the resilient response of granular materials. *Highway Research Record 345*, 15–31.

Khalili, N. and M. H. Khabbaz (1998). A unique relationship for χ for the determination of the shear strength of unsaturated soils. *Géotechnique 48*(5), 681–687.

Krahn, J. and D. G. Fredlund (1972). On total, matric and osmotic suction. *Soil Science 114*(5), 339–348.

Moran, M. J. and H. J. Shapiro (1996). *Fundamentals of Engineering Thermodynamics*. New York: Wiley and Sons.

Muraleetharan, K. K. and C. Wei (1999). Dynamic behaviour of unsaturated porous media: governing equations using the theory of mixtures with interfaces (TMI). *International Journal for Numerical and Analytical Methods in Geomechanics 23*, 1579–1608.

Pestana, J. M. and A. J. Whittle (1999). Formulation of a unified constitutive model for clays and sands. *International Journal for Numerical and Analytical Methods in Geomechanics 23*, 1215–1243.

Russo, M. A. (2000). Laboratory and field tests on aggregate base material for Caltrans accelerated pavement testing goal 5. Master's thesis, University of California at Berkeley.

Schofield, A. N. (1998). The "Mohr-Coulomb"error. *Mechanics and Geotechnique, LMS Ecole Polytechnique 23*, 19–27.

Seed, H. B., C. K. Chan, and C. E. Lee (1962). Resilience characteristics of subgrade soils and their relation to fatigue failures in asphalt pavements. In *International Conference on the Structural Design of Asphalt Pavements*, University of Michigan, Ann Arbor, pp. 611–636.

Swarbrick, G. E. (1995). Measurement of soil suction using the filter paper method. In *1st International Conference on Unsaturated Soils*, Paris, France.

Theyse, H. L. (2000). The development of mechanistic-empirical permanent deformation design models for unbound pavement materials from laboratory and accelerated pavement test data. In *5th International Symposium on Unbound Aggregates in Roads, A. R. Dawson (Ed.)*, Nottingham, U.K., pp. 285–293.

Uzan, J. (1985). Characterization of granular material. *Transportation Research Record 1022*, 52–59.

Van Genuchten, M. T. (1980). A closed-form equation for predicting the hydraulic conductivity of unsaturated soils. *Soil Science Society of America Journal 44*, 892–898.

Zienkiewicz, O. C., A. H. C. Chan, M. Pastor, B. A. Schrefler, and T. Shiomi (1999). *Computational Geomechanics with Special Reference to Earthquake Engineering*. Chichester, U.K.: Wiley and Sons.